NPS ARCHIVE
1964
ANDRESS, W.

Thesis
A497

U. S. Naval Postgraduate School
Monterey, California

DUDLEY KNOX LIBRARY
NAVAL POSTGRADUATE SCHOOL
MONTEREY CA 93943-5101

POLARIZATION OF NEUTRONS FROM THE $Li^7(p,n)Be^7$ REACTION FOR 3 TO 4 MeV PROTONS

by

William Dozier Andress, Jr.
Lieutenant (junior grade)
United States Navy

U. S. Naval Postgraduate School
Monterey, California

DUDLEY KNOX LIBRARY
NAVAL POSTGRADUATE SCHOOL
MONTEREY CA 93943-5101

ACKNOWLEDGMENTS

I would like to express my appreciation to Dr. R.L. Walter, my research director, for his guidance and assistance, to Messrs. J.R. Sawers, F.O. Purser and G.L. Morgan for their support in taking the data, to Mrs. J.R. Bailey for her preparation of the illustrations, and to my wife Kay for her assistance in analyzing the data.

This work was supported in part by the United States Atomic Energy Commission, the National Science Foundation, and the United States Navy.

W.D.A.

CONTENTS

ACKNOWLEDGMENTS ii

LIST OF FIGURES iv

LIST OF TABLES v

I. INTRODUCTION 2

II. THEORY 7

III. EXPERIMENTAL APPARATUS AND PROCEDURE 14

Accelerator and Targets, 14
A Typical Analyzing System, 15
Detectors, 18
Scatterer, 19
Electronics, 23
Solenoid, 27
Summary of the Method, 30

IV. ANALYSIS OF DATA AND THE RESULTS 36

Calculation of $\overline{F}_2$, 36
Determination of ^{2}True Asymmetry, 44

V. DISCUSSION AND CONCLUSIONS 53

APPENDIX 61

LIST OF REFERENCES 65

LIST OF FIGURES

1. Summary of Previous Experiments on the Polarization of Neutrons Emitted in the Reaction $Li^7(p,n)Be^7$. 5

2. Geometry of Double Scattering Polarization Experiments. 10

3. Typical Arrangement for Measuring $Li^7(p,n)Be^7$ Neutron Polarization. 17

4. High Pressure Thin-Walled Helium Cell. 22

5. Block Diagram of the Electronic Apparatus. 26

6. Physical Arrangement of the Solenoid and Its Performance in Creating a Uniform Longitudinal Field. 32

7. Actual Arrangement Used to Measure the Polarization of Neutrons. 35

8. Efficiency of the Plastic Scintillator. 39

9. Geometry Involved in the Computation of $\bar{F}_p$. 41

10. Pulse-Height Spectrum of the Helium Recoils in the Helium Cell. 48

11. Elimination of the First-Excited-State Group of Neutrons from the Asymmetry. 50

12. Polarization of Neutrons in the Region T_p = 3.0 to 4.0 MeV. 55

LIST OF TABLES

1. Multiple Scattering in the Helium Cell 45

2. Results of Measurements and Calculations 51

POLARIZATION OF NEUTRONS FROM THE $Li^7(p,n)Be^7$ REACTION FOR 3 TO 4 MeV PROTONS

Chapter I

INTRODUCTION

Because of its widespread use as a monoenergetic neutron source of variable energy, nearly all phases of the reaction $Li^7(p,n)Be^7$ have been investigated thoroughly (Gibbons and Newson, 1960). Measurements of the value of the polarization of these neutrons, i.e., the degree of systematic orientation of their spins, began in 1954 (Willard, Bair, and Kington, 1954; Adair, Darden, and Fields, 1954). Because the cross section for this reaction is large and the polarization of the emitted neutrons is high, the reaction since has served as the most frequently used source of polarized neutrons. As an example of its use, Elwyn and Lane recently determined the magnitude of the spin-orbit interaction for neutron scattering from seven light nuclei (1962) and Elwyn et al. for four heavy ones (1964). A source of neutrons with well defined polarization is essential to this type of scattering experiment.

Experiments to determine the polarization produced in this reaction have been performed at proton energies from just above threshold at 1.881 MeV to 10 MeV. For energies below 5 MeV the polarization has been obtained most extensively for

$\theta_l = 50°$ [#] at which emission angle the polarization is relatively high. The value of the polarization at this angle is fairly well known except in the region from about 3 to 4 MeV (Figure 1). In this region no extensive, high-accuracy experiments have been conducted previously. One expects that rapid variations may occur in the polarization at the energies near narrow resonances in reaction cross sections such as at 2.25 MeV in the $Li^7(p,n)Be^7$ reaction. This indeed was observed by Elwyn and Lane (1962). Above 4 MeV the results of experiments by Baicker and Jones (1960) and Benenson, May, and Walter (1962) are consistent with the effect of the broad resonance at about 5 MeV. It is well known that the total cross section is essentially constant in the 3 to 4 MeV region (Gibbons and Newson, 1960). Because no narrow resonances have been observed in this region, it is to be expected that large fluctuations in the polarization will not occur. However, in the 3 to 4 MeV region the reported values of polarization are statistically inconsistent with this expectation. The summary of the measurements shown in Figure 1 indicates large rapid variations. If one considers only the Baicker and Jones (1960) values, a slow variation generally is observed. However, due to the large statistical and systematic uncertainties, which were quoted by these authors, the actual magnitude of the polarization is somewhat undetermined. Conclusions drawn from experiments which employed the $Li^7(p,n)Be^7$ reaction as a source of polarized neutrons had to be tempered by these uncertainties and discrepancies.

[#] All angles and energies are in the laboratory system unless otherwise specified.

Figure 1

Summary of Previous Experiments on the Polarization of Neutrons Emitted in the Reaction $Li^7(p,n)Be^7$. All data was taken at an angle 50^0 relative to the proton beam axis except that of Elwyn and Lane which was taken at 51^0.

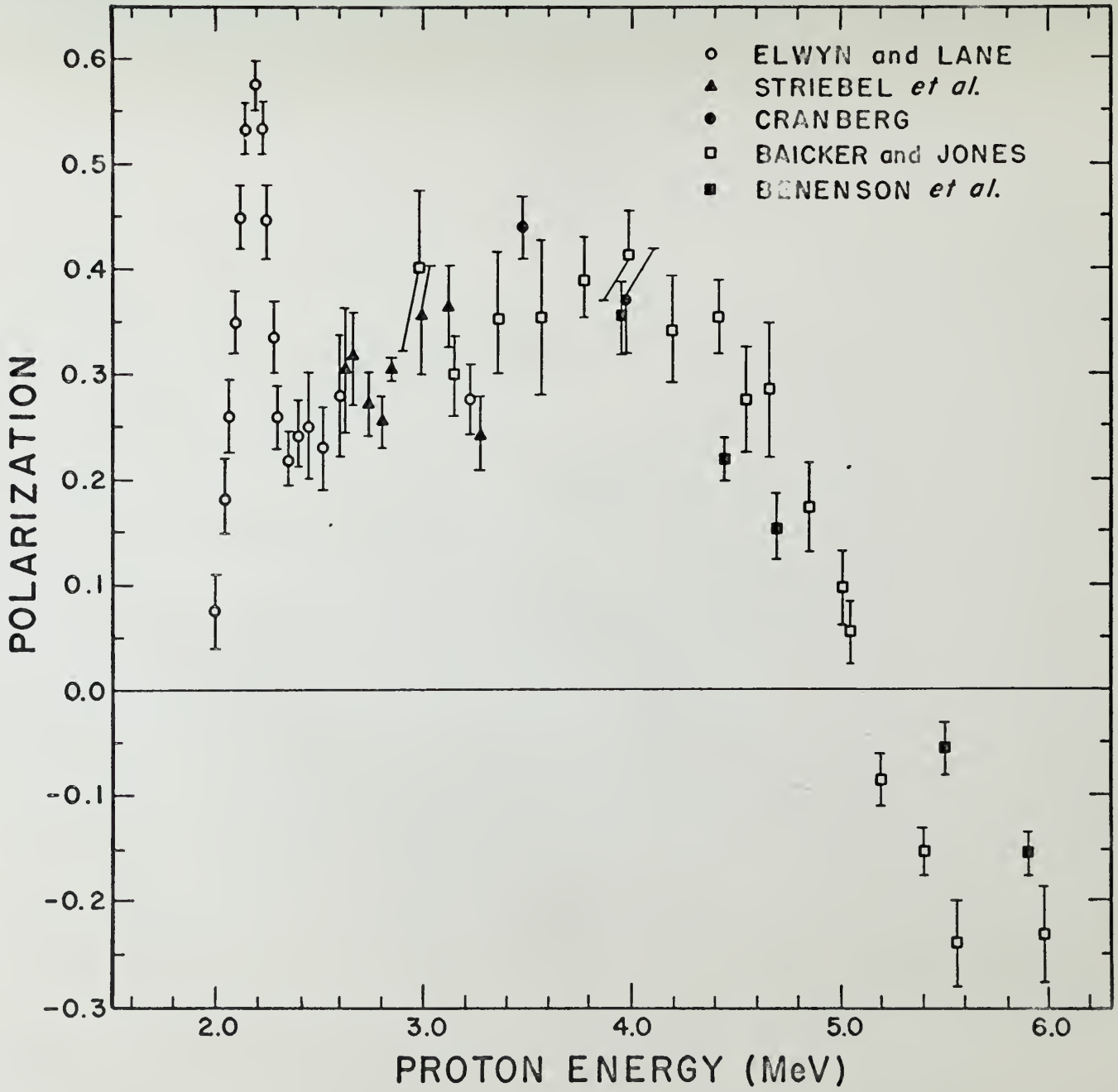
ELWYN and LANE
STRIEBEL et al.
CRANBERG
BAICKER and JONES
BENENSON et al.
POLARIZATION
0.6
0.5
0.4
0.3
0.2
0.1
0.0
-0.1
-0.2
-0.3
2.0
3.0
4.0
5.0
6.0
PROTON ENERGY (MeV)

In order to clarify this situation, accurate measurements were made at six energies in the region 3 to 4 MeV at a reaction angle of 50°. A solenoid was used to rotate the polarization vector $\vec{P}_1$ of the neutron beam so that mechanical asymmetries, which arise due to the usual rotation of the detectors, were eliminated. Elastic scattering from helium enclosed at high pressure in a thin-walled cell was used as an analyzer. By requiring a coincidence between the helium scattered neutrons and the recoil alpha particles, background was reduced to about 5 percent.

Chapter II

THEORY

The formal theory of polarization of nucleon beams is entirely quantum mechanical in nature and cannot be explained successfully by semiclassical reasoning. Since a presentation of the theory at this level is beyond the scope of this paper, the theoretical results and an explanation of the principles as they apply to the present experiment will be the primary subjects of this chapter. The reader who is interested in a detailed discussion of the general theory can consult Welton (1963) whose treatment of the topic is general and thorough. Very limited, but more easily understood discussions are to be found in advanced nuclear physics texts. (See for example Bethe and Morrison [1956] and Preston [1962].)

Polarization of nuclei and nucleons refers to the orientation in space of their spins. A beam of neutrons is polarized if the spins have a preferred direction in space as opposed to random ordering. Any nucleon beam can be looked upon as being comprised of a combination of two spin states which are referred to as spin-up and spin-down with respect to a given axis. The degree of polarization is defined as

$$P_1 = (N_+ - N_-)/(N_+ + N_-) \qquad (1)$$

where N_+ refers to those neutrons with spin-up and N_- to those with spin-down.

In the case of polarization in elastic scattering, which corresponds closely to polarization in reactions, the polarization of the scattered neutrons can be predicted by optical model theory if a spin-orbit term is added to the potential used to describe the interaction. There is a general agreement between predicted polarizations and experimental values, but precise quantitative results as yet have not been obtained. It is interesting to note that "spin-orbit coupling in the shell model is of the same sign and approximately the same magnitude as that used to calculate polarizations in the optical model" (Emmerich, 1963).

Both the incident protons and the target nuclei are normally unpolarized in a reaction X(p,n)Y. However, the outgoing neutrons are usually polarized because of the strong spin-orbit coupling in nuclear reactions (Haeberli, 1963). In contrast with the corresponding coupling in the case of atomic electrons, the nuclear spin-orbit interaction is not electromagnetic in origin (Eisberg, 1961). The interaction is a result of nuclear forces but is not well understood. Due to spin-orbit coupling, interference occurs between different partial waves involved in the reaction; polarization results.

In the reaction X(p,n)Y the magnitude of the polarization depends upon both the proton energy and the reaction angle θ_1 (Figure 2). The degree of polarization can be expressed as

Figure 2

Geometry of Double Scattering Polarization Experiments. Monoenergetic charged particles are incident on the target. Those neutrons which are emitted at an angle θ_1 are incident on the scattering sample. In turn neutrons which are deflected through an angle θ_2 are detected at $\varphi = 0$ and $\varphi = \pi$, where φ is the angle between the unit vectors $\vec{n}_1$ and $\vec{n}_2$. These unit vectors are in the direction $\vec{k}_p \times \vec{k}_n$ and $\vec{k}_n \times \vec{k}'_n$ respectively where the $\vec{k}_i$ are the momentum vectors of the charged particles and the emergent and scattered neutrons.

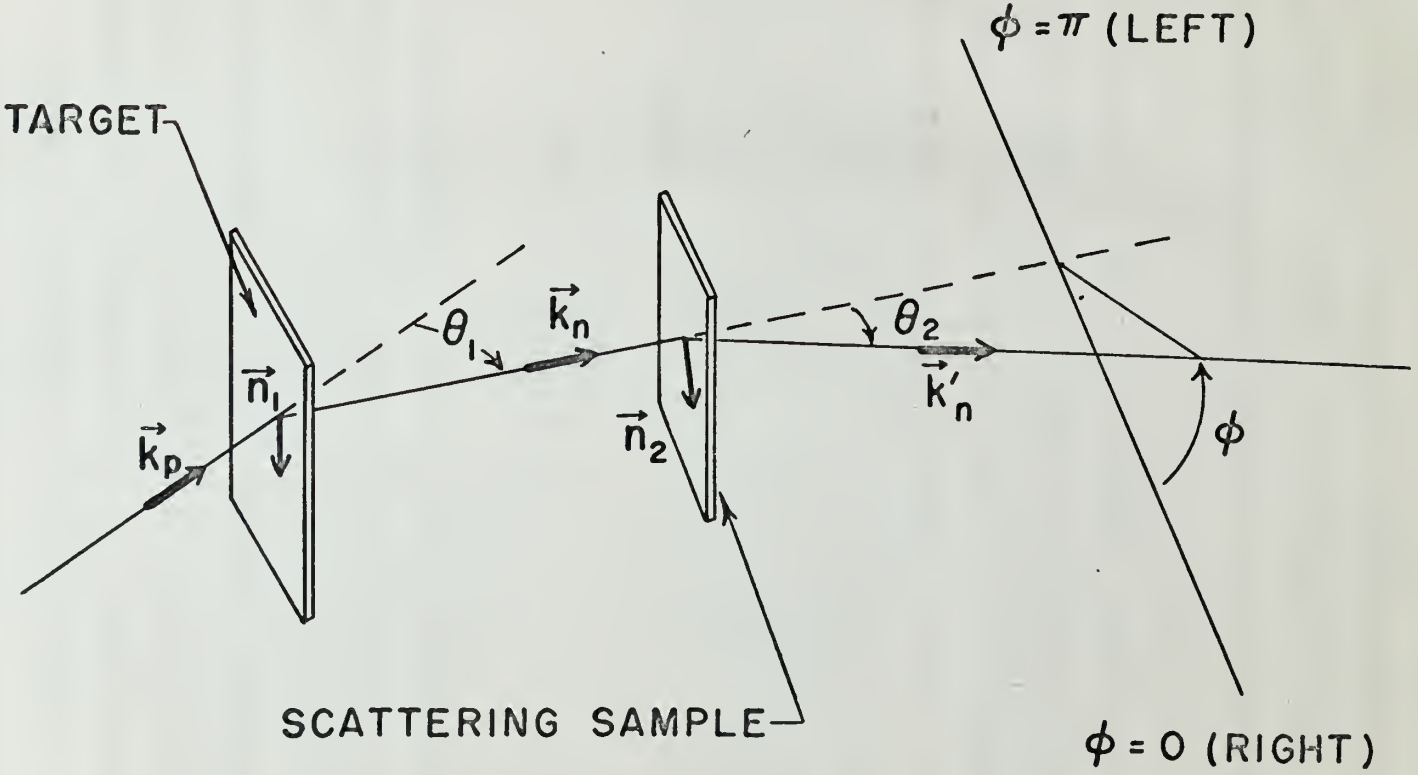
TARGET
$\vec{k}_p$
$\vec{n}_1$
θ_1
$\vec{k}_n$
$\vec{n}_2$
θ_2
$\vec{k}'_n$
ϕ
$\phi = \pi$ (LEFT)
$\phi = 0$ (RIGHT)
SCATTERING SAMPLE

(Haeberli, 1963)

$$P_1(\theta_1) = [1/\sigma(\theta_1)] \sum_{L=1}^{L_{max}} A_L P_L^{(1)}(\theta_1) \qquad (2)$$

where $\sigma(\theta_1)$ is the differential reaction cross section and $P_L^{(1)}(\theta_1)$ are the associated Legendre polynomials. The A_L are complicated coefficients which depend upon the reaction. The upper limit on the index of summation is dependent upon the largest effective value of the total angular momentum and the incident and final values of the orbital angular momentum. From symmetry arguments it can be shown that the polarization produced in the outgoing neutron beam is perpendicular to the plane which contains the initial and final momentum vectors, the so-called reaction plane. The positive direction of polarization is a matter of definition and in accordance with the Basel Convention (Sign, 1960) will be taken as

$$\vec{n}_1 = \frac{\vec{k}_p \times \vec{k}_n}{|\vec{k}_p \times \vec{k}_n|} \quad , \qquad (3)$$

where the $\vec{k}$ represents the momentum vector of the particle and the subscripts refer to the incident proton and outgoing neutron.

Since neutron detectors are insensitive to the orientation of the spin vector, one cannot measure the polarization directly. The scattering of unpolarized beams is azimuthally symmetric about the incident beam axis, but the differential cross section for scattering polarized neutrons depends on the azimuthal angle φ. This property of nuclear elastic scattering can be utilized to detect polarization in a neutron beam.

The sensitivity of nuclear elastic scattering to the polarization of the incident beam is called the analyzing power of the scatterer. The analyzing power P_2 is defined properly as the polarization which would result in the elastic scattering of an initially unpolarized beam. Its direction is

$$\vec{n}_2 = \frac{\vec{k}_n \times \vec{k}'_n}{|\vec{k}_n \times \vec{k}'_n|} \tag{4}$$

where the prime denotes the scattered neutron. The differential cross section for the scattering of polarized neutrons is (Haeberli, 1963)

$$\sigma(\theta_2, \varphi) = \sigma(\theta_2)(1 + \vec{P}_1 \cdot \vec{P}_2) . \tag{5}$$

If measurements of neutron intensities are made at $\varphi = 0$ (right) and $\varphi = \pi$ (left), from Equation (5) it follows that

$$r = I_0/I_\pi = (1 + P_1P_2)/(1 - P_1P_2) \tag{6}$$

which directly yields

$$P_1P_2 = (r - 1)/(r + 1); \tag{7}$$

r is called the right-left ratio.

Since in determining the polarization one can measure only the asymmetry P_1P_2, he must know or be able to calculate the analyzing power P_2. This is one of the most critical problems in any polarization experiment. For most nuclei the analyzing power is still unknown. P_2 can be calculated whenever the scattering phase shifts are known, and they are best known for light, spinless nuclei. For this reason He^4, C^{12}, and O^{16}

are used most often as polarization analyzers. For these spin-zero nuclei, the partial wave corresponding to a given orbital angular momentum can have only two phase shifts, δ_ℓ^+ corresponding to $j = \ell + \frac{1}{2}$ and δ_ℓ^- to $j = \ell - \frac{1}{2}$. When elastic scattering is the only process involved, the phase shifts are real. In the particular case of spin-zero nuclei, the polarization becomes (Haeberli, 1963)

$$P_2 = -2\,\mathrm{Im}(g^* h) / (|g|^2 + |h|^2) \qquad (8)$$

where

$$g = (1/k) \sum_\ell P_\ell(\cos\theta) \left[(\ell+1) \sin\delta_\ell^+ \exp(i\delta_\ell^+) + \ell \sin\delta_\ell^- \exp(i\delta_\ell^-) \right],$$

$$h = (1/k) \sum_\ell P_\ell^{(1)}(\cos\theta) \sin(\delta_\ell^+ - \delta_\ell^-) \exp(i\delta_\ell^+ + i\delta_\ell^-),$$

k is the neutron wave number, ℓ is the orbital angular momentum quantum number, and $P_\ell(\cos\theta)$ and $P_\ell^{(1)}(\cos\theta)$ are the ordinary and associated Legendre polynomials respectively. It should be noted that the denominator is just the differential cross section and that this result is of the form of Equation (2). If errors exist in the phase shifts, they are correlated in a complicated way in Equation (8). Because of this it is very difficult to estimate the accuracy of the analyzing power determined in this manner.

Chapter III

EXPERIMENTAL APPARATUS AND PROCEDURE

The apparatus peculiar to polarization measurement which was used in this experiment was designed by F.O. Purser and J.R. Sowers of this laboratory.

Accelerator and Targets

Protons were accelerated by the Duke University 4.0 MeV Van de Graff electrostatic generator and were momentum analyzed by an electromagnetic filter. The resulting monoenergetic proton beam was incident on a lithium target. A precision digital voltmeter with a generating voltmeter was used to determine the proton energy. This system is linear over the region investigated and is very stable (Hollandsworth, Buccino, and Bevington, 1964). The digital voltmeter was calibrated several times during the course of the experiment using the known threshold at 1.881 MeV for the $Li^7(p,n)Be^7$ reaction.

The lithium targets were prepared by evaporating lithium flouride onto tantalum backing or "end caps". Target thicknesses were determined by the rise curve method (Taschek and Hemmendinger,

1948). Targets averaging about 80 keV to protons at the energy of the particular measurement were employed. Because of the relatively large proton current of five microamperes, it was necessary to cool the targets by spraying water onto the outside of the end cap. The end caps were soaped at frequent intervals to prevent minerals in the water from depositing on them.

A Typical Analyzing System

A typical arrangement for measuring polarization is shown in Figure 3. This is not the system which was used in the present experiment, but this setup forms the basis about which our apparatus was designed.

In order to measure the asymmetry the neutrons which were emitted at an angle θ_1 from the reaction $Li^7(p,n)Be^7$ are incident on a scattering sample as shown. The detector is rotated from the $\varphi = 0$ (right) to the $\varphi = \pi$ (left) position. In each position the neutron intensities are measured; the asymmetry is determined from Equation (7),

$$P_1 P_2 = (r - 1)/(r + 1) , \qquad (7)$$

where $r = I_0 / I_\pi$. This method requires that a beam monitor be used so that the same number of protons is incident on the lithium target for each measurement of intensity. A current integrator can be used for this purpose.

Figure 3

Typical Arrangement for Measuring $Li^7(p,n)Be^7$ Neutron Polarization.

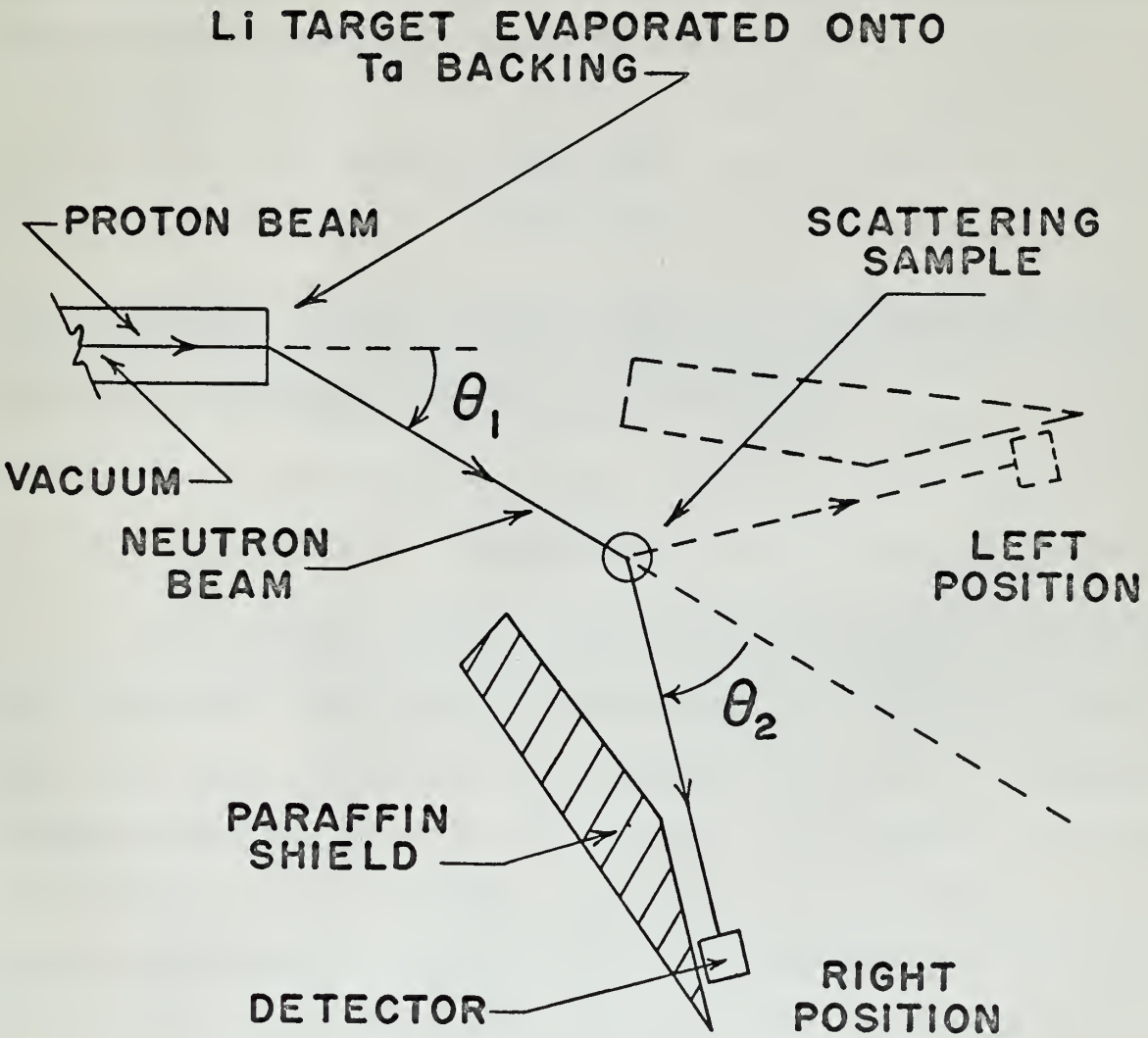
Li TARGET EVAPORATED ONTO
Ta BACKING
PROTON BEAM
SCATTERING
SAMPLE
θ_1
VACUUM
NEUTRON
BEAM
LEFT
POSITION
θ_2
PARAFFIN
SHIELD
DETECTOR
RIGHT
POSITION

The time for recording a given amount of data can be halved if two detectors are used rather than one. In the "typical arrangement" they would be mounted at $\varphi = 0$ and $\varphi = \pi$. The detectors probably will not have the same detection efficiency; however, the efficiencies cancel completely if the detectors are rotated and the right-left ratio is taken as

$$r = \sqrt{\frac{I_{r,1}}{I_{\ell,1}} \times \frac{I_{r,2}}{I_{\ell,2}}} \quad . \tag{7}$$

The subscripts r and ℓ indicate right and left positions and the numerals arbitrarily indicate the detectors.

Detectors

The neutron detectors which were used employ NE 102 plastic phosphor.[#] This organic scintillator was selected because of its short decay time, non-susceptibility to shock and relative inexpensiveness. In a plastic phosphor the neutrons are detectable because of the ionizing properties of the recoiling light nuclei--principally hydrogen. Due to the isotropy of the n-p scattering cross section for neutrons of the energy range involved in this work, the energies of the recoil protons are distributed uniformly. Because the light output from the carbon recoils is relatively small, the carbon does not affect the performance of

---

[#]The detectors were obtained from Nuclear Enterprises Ltd.

the detector in this experiment.

The detectors, which were 5.08 x 5.08 x 2.54 cm in size, were wrapped on five sides with aluminum foil which acted as a light reflector. A 0.5 cm thick lead shield for attenuation of gamma radiation also surrounds the scintillator. An RCA 6810 longitudinal photomultiplier tube viewed the scintillator through a Lucite light pipe which closed the otherwise open end. The purpose of a light pipe is to permit the location of the photomultiplier tube out of stray magnetic fields. This fourteen stage photomultiplier tube was selected because of its large output pulse, which is needed for fast coincidence work. The phototubes were surrounded by a mu-metal cylinder of 0.16 cm thickness and were mounted in 0.95 cm thick armco iron outer cylinders to further reduce the effects of stray magnetic fields and to serve as supports for the tubes. Discriminators permitted only pulses corresponding to 210 keV energy or greater to be counted.

Scatterer

The sample which was employed to scatter the neutrons differed appreciably from the usual slab or cylinder. Gaseous helium which was enclosed in a stainless steel container served as the scatterer. There are two reasons for using helium. It is a spin-zero light nucleus for which the scattering phase shifts are relatively well known. As previously discussed, the analyzing power can be calculated in this case. Also, the recoil alpha particles

cause scintillations which can be seen readily with a photomultiplier tube. This permits the use of coincidence techniques. Requiring a coincidence between the pulses in the plastic scintillators due to the helium-scattered neutrons and the recoil helium scintillations greatly reduces background.

The helium cell was patterned after one reported by R.E. Shamu (1962). It was constructed of type 304 stainless steel, 0.22 cm thick. The cell is a cylinder with a basically hemispherical closed end (Figure 4). The interior of the cell is coated with a thin layer of aluminum upon which a 0.1 cm layer of MgO is deposited. The purpose of these layers is to reflect the light of the helium scintillations. The open end of the cell is closed by a tempered plate glass disc and a Lucite light pipe which give a window to view the scintillations. A Teflon O-ring is used for a seal between the glass and steel. A thin layer of diphenyl stilbene was deposited on the MgO and the glass window to serve as a wavelength shifter. The cell was filled with a helium-xenon gas mixture in a proportion of four atmospheres of xenon to 102 atmospheres of helium.

The mechanism by which the helium cell detects neutrons has not been completely explained (Huddleston, 1960). As it is presently understood, the neutrons lose an appreciable amount of their energy to the helium atoms. The resulting alpha particles lose their kinetic energy primarily by electromagnetic interaction with the electrons of the xenon atoms resulting in ionization and excitation of the xenon. Recombination and deexcitation, with

Figure 4

High Pressure Thin-Walled Helium Cell.

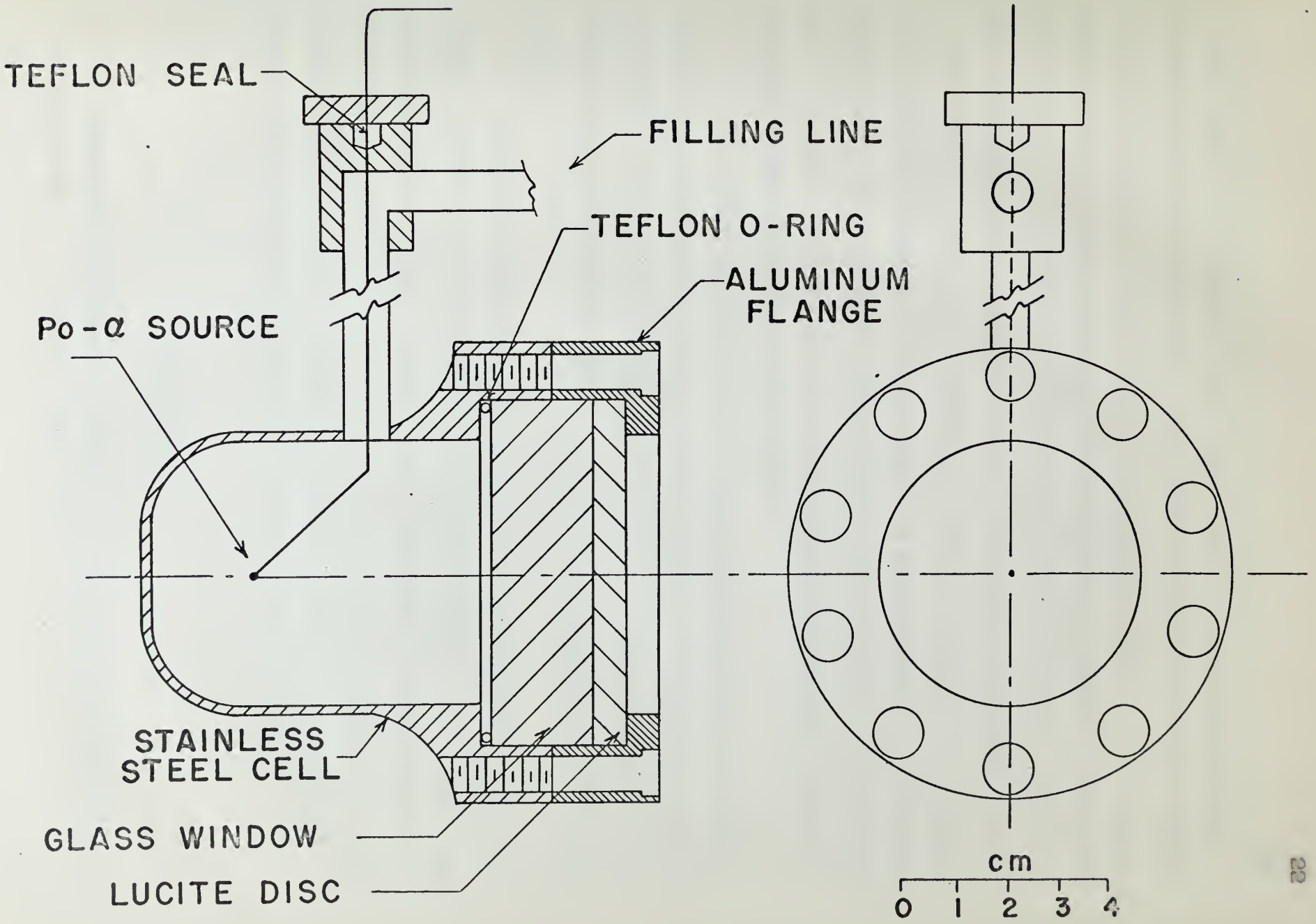
TEFLON SEAL
FILLING LINE
TEFLON O-RING
ALUMINUM FLANGE
Po-α SOURCE
STAINLESS STEEL CELL
GLASS WINDOW
LUCITE DISC
cm
0 1 2 3 4

their associated light of emission, follow. The scintillation pulses observed consist of a long lived (slow) and a short lived (fast) component. Presumably recombination, which is a relatively slow process, accounts for the slow component observed, and deexcitation, a much faster process, accounts for the fast component. If the deexcitation process is one of resonance radiation, one expects that the resonance radiation would be recaptured and reemitted many times before it could reach the photocathode. This would result in a longer lived component than is observed. Deexcitation of the xenon atoms causes the fast pulse, but the role played by resonance radiation is questionable.

The light emitted in the deexcitation process has a different band of frequencies from that to which the photocathode is sensitive. The diphenyl stilbene coating is used to convert the frequencies of the photons to those of the photocathode sensitive region.

To allow a determination of the energy resolution of the cell, a Po^{210} alpha source was introduced through the filling line as shown in the figure. Helium cell resolution is defined to be the energy spread of the peak in the pulse-height spectrum of the alpha particles at half maximum height divided by the particle energy. The resolution was determined to be 15 percent.

Electronics

Each time a neutron interacts in the plastic scintillator

or the helium cell, a pulse is generated in the corresponding phototube. A block diagram of the apparatus for converting these signals into meaningful data is shown in Figure 5.

Pulses with fast rise times originate at the plate of the phototubes of the helium cell and detectors. They are amplified in Hewlett-Packard wide band amplifiers which limit the pulses to eight volts. Delay line clipping is employed to shape the pulses uniformly to a 10 nsec width. These 10 nsec pulses are the inputs to the fast coincidence circuit which is a modification of one proposed by R.H. Miller (1959). Anytime a signal appears in a detector coincident with one from the helium cell, a pulse is transmitted from the fast coincidence circuit associated with that detector to the appropriate triple coincidence circuit. The double pulse resolving time of the fast coincidence circuit is about 10 nsec.

The fact that a scintillation is seen by the neutron phototube coincident with one in the helium cell phototube does not require that these be caused by the same neutron or even by neutrons. One or both of the pulses may have been due to a background neutron or a gamma ray. When a neutron is scattered through a specific angle, the kinematics of elastic scattering requires that the neutrons transfer a definite amount of their energy to the alpha particle and retain the remaining portion. In order to use this property beneficially, triple coincidence techniques are incorporated. Inputs to the triple coincidence circuit originated at the eleventh dynodes of the phototubes of either the helium cell or the neutron detector. A Hamner 303 amplifies the helium recoil pulses

Figure 5

Block Diagram of the Electronic Apparatus.

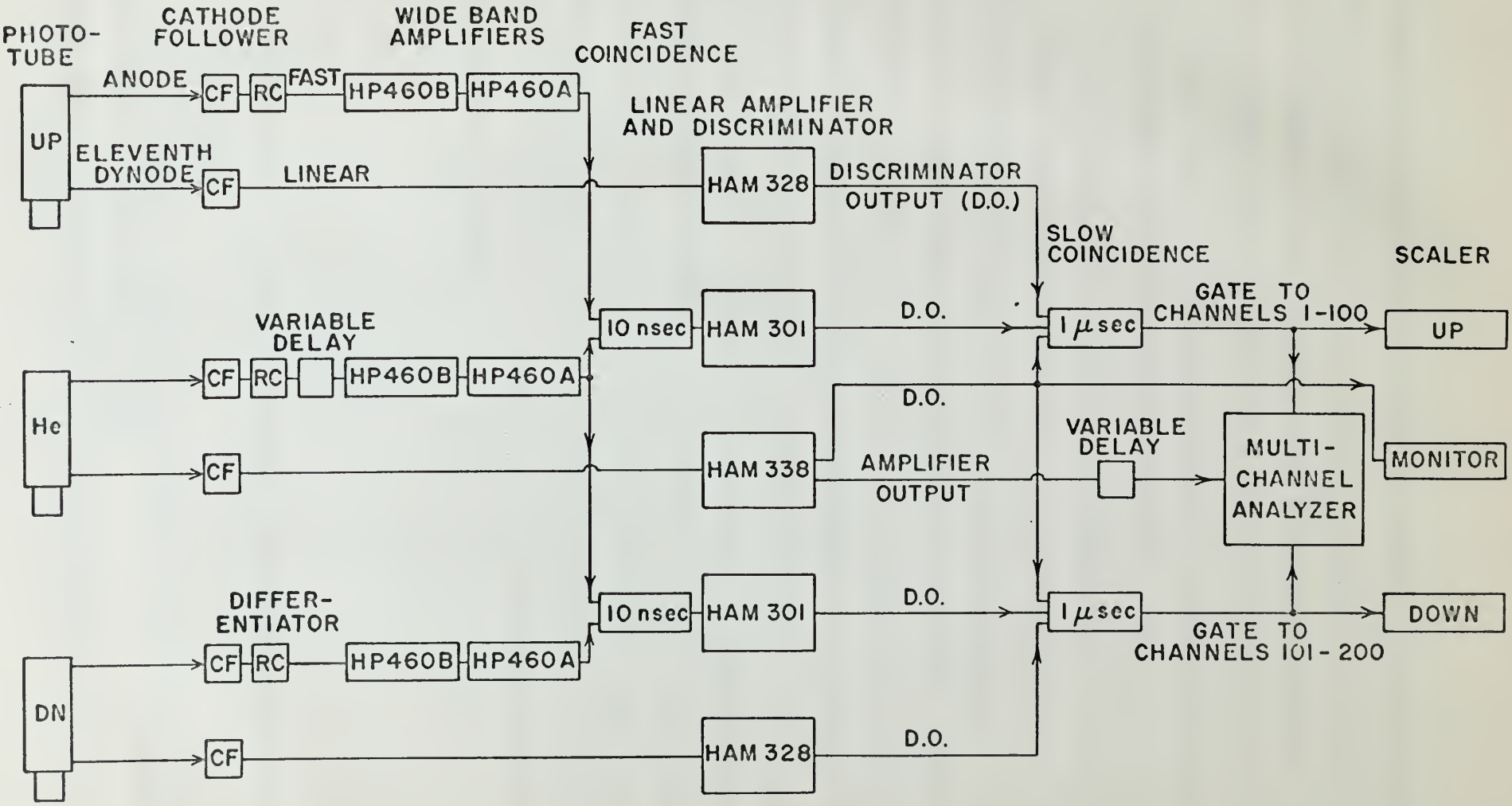
PHOTO-TUBE
CATHODE FOLLOWER
WIDE BAND AMPLIFIERS
FAST COINCIDENCE
ANODE
CF
RC
FAST
HP460B
HP460A
UP
ELEVENTH DYNODE
CF
LINEAR
LINEAR AMPLIFIER AND DISCRIMINATOR
HAM 328
DISCRIMINATOR OUTPUT (D.O.)
SLOW COINCIDENCE
SCALER
VARIABLE DELAY
10 nsec
HAM 301
D.O.
1 μsec
GATE TO CHANNELS 1-100
UP
He
CF
RC
HP460B
HP460A
CF
D.O.
HAM 338
AMPLIFIER OUTPUT
VARIABLE DELAY
MULTI-CHANNEL ANALYZER
MONITOR
DIFFER-ENTIATOR
10 nsec
HAM 301
D.O.
1 μsec
DOWN
GATE TO CHANNELS 101-200
DN
CF
RC
HP460B
HP460A
CF
HAM 328
D.O.

and a discriminator is triggered only by those pulses corresponding to neutrons which are scattered through a certain angle or greater. In order to obtain an output pulse from the slow coincidence circuit, three conditions must be satisfied. The detector pulse must correspond to a helium cell scintillation, and both the neutron and alpha pulses must be energetically acceptable. Amplified linear pulses from the helium cell, which are accompanied by a gate pulse from the "upper" slow coincidence circuit, are analyzed by a TMC Model 400* multichannel analyzer and stored in channels 1 - 100, those from the "lower" circuit in channels 101 - 200. This device examines the input pulse and records it in a specific channel which depends upon the height or energy of the pulse. The output of the analyzer is a plot of the number of pulses at a given energy as a function of the energy. In order to maintain a constant check on the performance of the electronics circuits and on target deterioration, EIDL 49-2* scalers were used to record the output of the slow coincidence circuits and the helium cell pulses. Typically, there were about 60 counts per minute per slow coincidence circuit registered by the scalers.

Solenoid

Since neutron detector efficiencies are difficult to

---

*The 400 channel analyzer was obtained from Technical Measurement Corp., North Haven, Conn.

*The Nuclear-Chicago Corp. of Melrose Park, Ill. manufactured these scalers.

determine absolutely, it is necessary to interchange the detectors on either side of the beam to measure an asymmetry whether one or two detectors are used in the "typical arrangement". This interchange is the weakness of the system. The scatterer to detector distance must be kept constant to avoid changing the detector solid angle subtended by the scatterer. Because of the anisotropies in the differential cross section, care also must be taken to place the detectors at the same angle on both sides of the beam. If the proper radial distance and angle are not maintained, false asymmetries are introduced into the measured quantity.

A method to eliminate these false asymmetries first was proposed and employed by Hillman, Stafford and Whitehead (1956). The method utilizes the rotation of the polarization vector of the neutron beam $\vec{P}_1$ through 90° by the Larmour precession of the magnetic moment in a uniform magnetic field produced by a solenoid. With the proper field $\vec{P}_1$ is rotated 90° about the beam axis into the plane perpendicular to the first reaction plane. The second reaction plane is now vertical and perpendicular to the first plane, and the detectors are fixed in this plane. A measurement of intensity is then taken in each detector. By reversing the field the polarization vector can be rotated 180° relative to the vector direction in which the first measurement was taken. This is entirely equivalent to moving the detector to the opposite side of the incident beam. The "right-left" ratio, Equation (9) becomes

$$r = \sqrt{\frac{I_{u,p}}{I_{u,a}} \times \frac{I_{d,a}}{I_{d,p}}} \qquad (10)$$

where the subscripts u and d refer to the up and down detectors and p and a to the field directions parallel and antiparallel to the momentum vector $\vec{K}_n$. False mechanical asymmetries no longer enter into the experiment, and detector efficiencies cancel. In fact, no beam monitor is necessary because only relative counting rates are measured when the data are analyzed in this manner. This method also permits more frequent "interchange" of the detectors than is practical with a physical interchange. This minimizes the effect of long term electronics drifts.

The Larmour frequency of precession of the neutron magnetic moment is

$$\nu = g\mu_n H/h \text{ cps} \tag{11}$$

where g is the nuclear g factor, μ_n is the nuclear magneton, H is the magnetic field, and h is Planck's constant. If the neutron velocity is V (cm/sec) and the path length of the neutron in the magnetic field is ℓ, the field required to rotate the magnetic moment through 90^0 is

$$H = Vh/(4g\mu_n \ell) . \tag{12}$$

If the field is that due to an infinitely long solenoid one requires

$$NI = 0.94 \times 10^5 \sqrt{E_n} \quad \text{amp-turns} \tag{13}$$

when the neutron energy E_n is measured in MeV.

The solenoid which was used in the present experiment is a modular, air-core solenoid with tape wound coils which are cooled by direct water contact with the edges of the copper tape.#

#The solenoid was constructed by Magnion, Inc. of Cambridge, Mass. and is a modification of their Plasmaflux model.

It has a 5.72 cm diameter core. The solenoid is composed of three modules enclosed in an Armco iron box on five sides. A 0.95 cm thick slab covers the top whereas the ends have a 3.15 cm thick cover. The bottom of the solenoid is open to provide space for cooling water and power supply connections. With the existing power supply--a 35 kilowatt, 325 ampere generator--the maximum central field strength is 7.8 kilogauss.

Although the use of the solenoid eliminates the aforementioned mechanical asymmetries, asymmetries caused by the reversal of the magnetic field could be introduced. The fringing field might have an effect on the phototubes. This effect was minimized as discussed in the section on detectors. Also the proton beam might be deflected and caused to hit different portions of the lithium target, resulting in a different target thickness for various solenoid currents. The field was carefully measured and the fringing field was determined to be less than one gauss in the vicinity of the phototubes and proton beam. This has a negligible effect on the proton beam. Because of the shielding employed, a field of this magnitude has no effect on the phototubes. Figure 6 indicates the physical configuration of the solenoid and the field produced by it.

Summary of the Method

All this may be better understood if it is tied together in a brief summary with a figure showing the actual apparatus

Figure 6

Physical Arrangement of the Solenoid and Its Performance in Creating a Uniform Longitudinal Field.

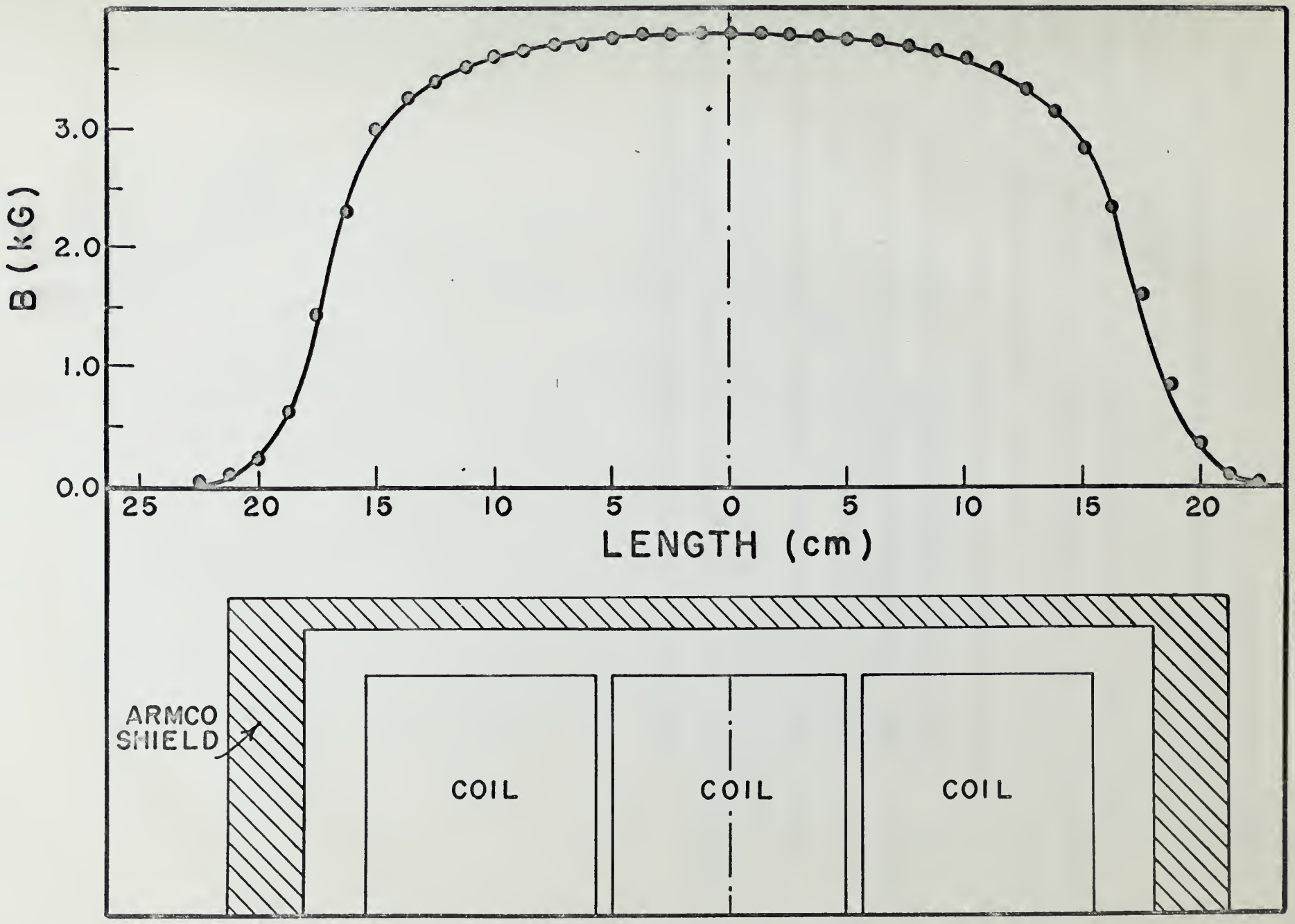
B (kG)
3.0
2.0
1.0
0.0
25
20
15
10
5
0
5
10
15
20
LENGTH (cm)
ARMCO
SHIELD
COIL
COIL
COIL

(Figure 7). Having been accelerated by the Van de Graff generator, the protons were incident on a lithium target. Those neutrons which emerged at a reaction angle of 50° relative to the proton beam axis had their polarization vectors rotated into the plane perpendicular to the first reaction plane by a longitudinal magnetic field produced with a solenoid. The neutrons were incident on a helium cell. Those which were scattered through an angle θ_2 were detected by a pair of plastic scintillators. For this work θ_2 was 100° or 120° depending upon which gave the greater value for P_2 at a particular neutron energy. Pulses caused by neutrons which were of the proper energy and which were coincident with helium recoils of the requisite energy were counted on scalers and were resolved by a multichannel pulse-height analyzer. The asymmetry was computed from Equations (7) and (10).

Figure 7

Actual Arrangement Used to Measure
the Polarization of Neutrons.

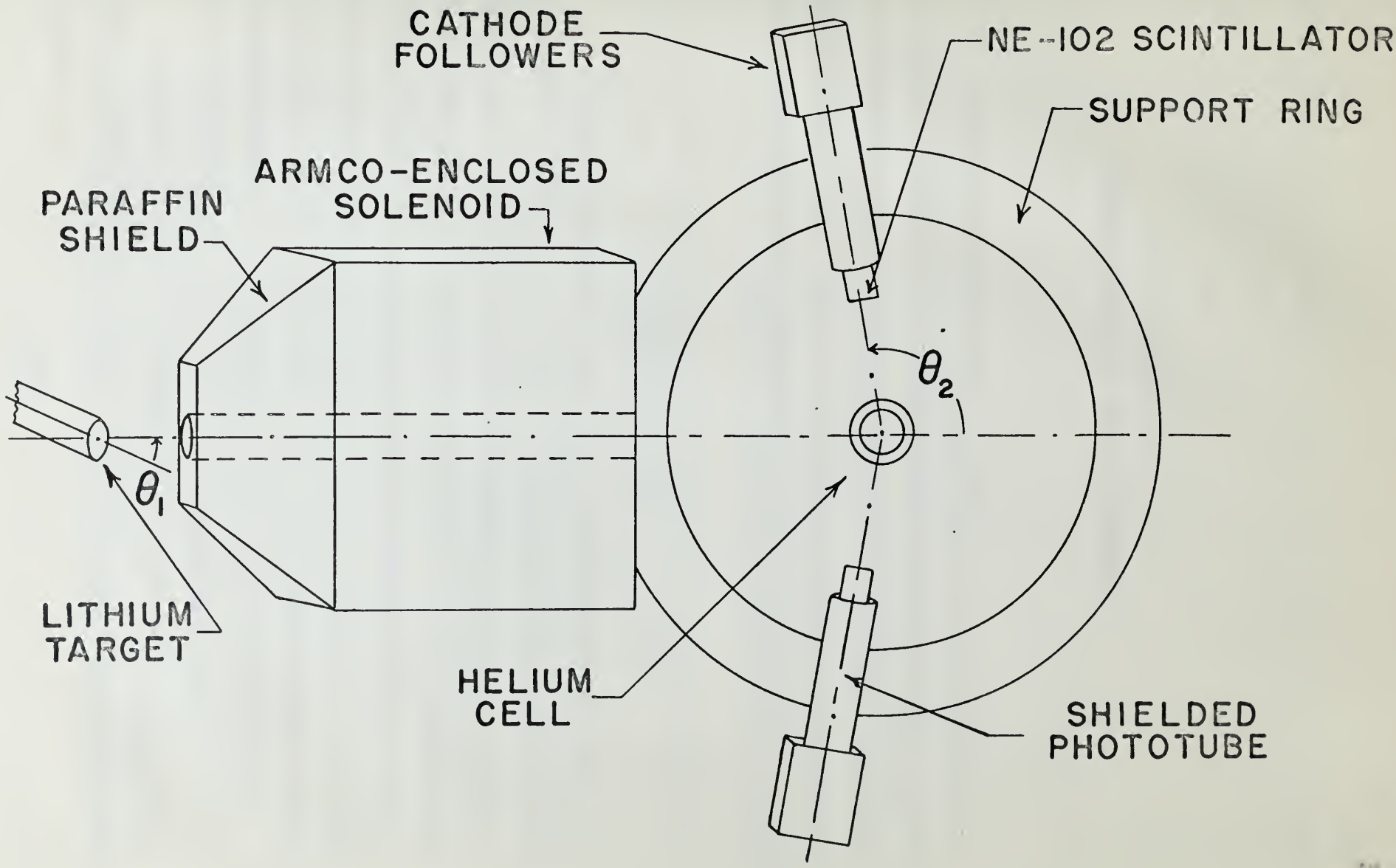
CATHODE FOLLOWERS
NE-102 SCINTILLATOR
SUPPORT RING
ARMCO-ENCLOSED SOLENOID
PARAFFIN SHIELD
θ_2
θ_1
LITHIUM TARGET
HELIUM CELL
SHIELDED PHOTOTUBE

Chapter IV

ANALYSIS OF DATA AND THE RESULTS

Analyzing the data was essentially a two-step process. The average value of the analyzing power of helium $\bar{P}_2(E_n, \theta_2)$ had to be determined for the various neutron energies and analyzing angles, and the true value of the asymmetry had to be established by the elimination of background and first excited state neutrons.

Calculation of $\bar{P}_2$

$\bar{P}_2(E_n, \theta_2)$ differs from $P_2(E_n, \theta_2)$ because of the geometry involved. Due to the finite sizes of the scatterer and detectors, effects such as multiple scattering and solid angles must be considered. It was assumed for the initial calculations that no multiple scattering of neutrons occurred in the helium cell or in the plastic detectors. $\bar{P}_2$ is a function of the efficiency of the neutron detectors $\eta(E_n)$, the differential scattering cross section for neutrons on helium $\sigma(\theta_2)$, the analyzing power of helium $P_2(E_n, \theta_2)$, and a geometric factor $f(\theta_2)$.

$P_2(E_n, \theta_2)$ and $\sigma(\theta_2)$ were determined from relations indicated in the previous chapter. In these calculations the phase

shifts of Dodder and Gammel, quoted by Seagrave (1953) were used.

The relative efficiency of the plastic scintillators is given by (Swartz and Owen, 1960)

$$\epsilon_1(E_n) = n_H \sigma_H L (1 - e^{-\alpha L})/\alpha L \qquad (14)$$

where n_H is the number of hydrogen atoms per cm^3 of scintillator, σ_H is the neutron-proton scattering cross section, L is the length of the scintillator, $\alpha = n_H \sigma_H + n_C \sigma_C$, n_C is the number of carbon atoms per cm^3 of scintillator, and σ_C the neutron-carbon cross section. The true efficiency for a biased detector can be calculated from

$$\eta(E_n) = (1 - B/E_n)\epsilon_1 \qquad (15)$$

where B is the bias energy. Those efficiency curves which were determined for this experiment are shown in Figure 8.

The geometric factor next was computed. To implement this the detectors were regarded as plane surfaces, and the helium cell and detectors were divided into eight sections (Figure 9). The probability of scattering from cell zone "i" into detector zone "j" is

$$f_{ij} = k \times \text{area}(j) \times \text{volume}(i) \times \exp(-\ell_i/\lambda)/r_{ij}^2 . \qquad (16)$$

From cell segment "i" to detector segment "j" the distance is r_{ij}; the path length in the cell before reaching volume (i) is ℓ_i; λ is the mean free path; k is a constant. The scatterer to detector distance was 17.4 cm so that r_{ij} was approximately a constant.

Figure 8

Efficiency of the Plastic Scintillator.

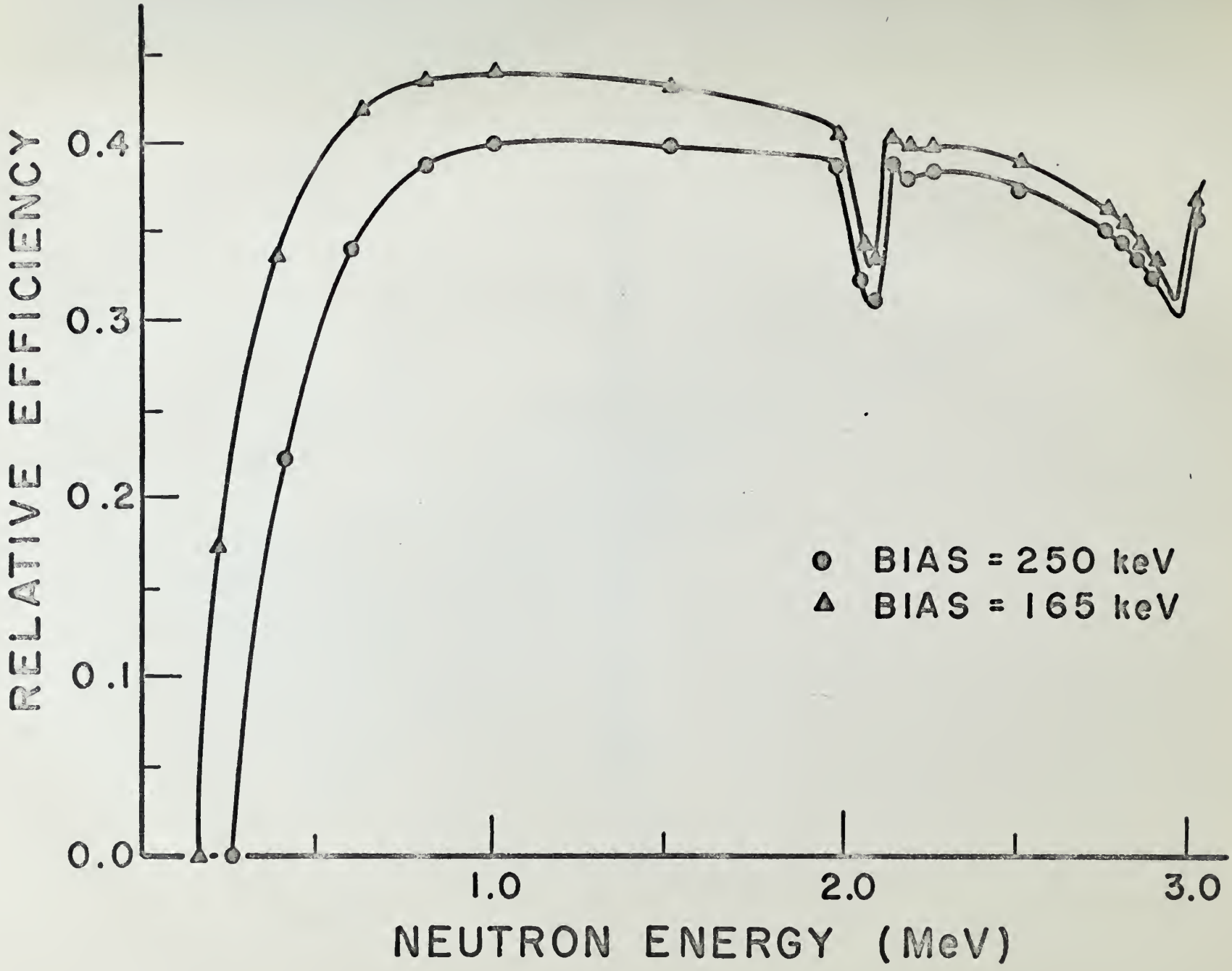
RELATIVE EFFICIENCY
0.0
0.1
0.2
0.3
0.4
1.0
2.0
3.0
NEUTRON ENERGY (MeV)
BIAS = 250 keV
BIAS = 165 keV

Figure 9

Geometry Involved in the Computation of F_2.

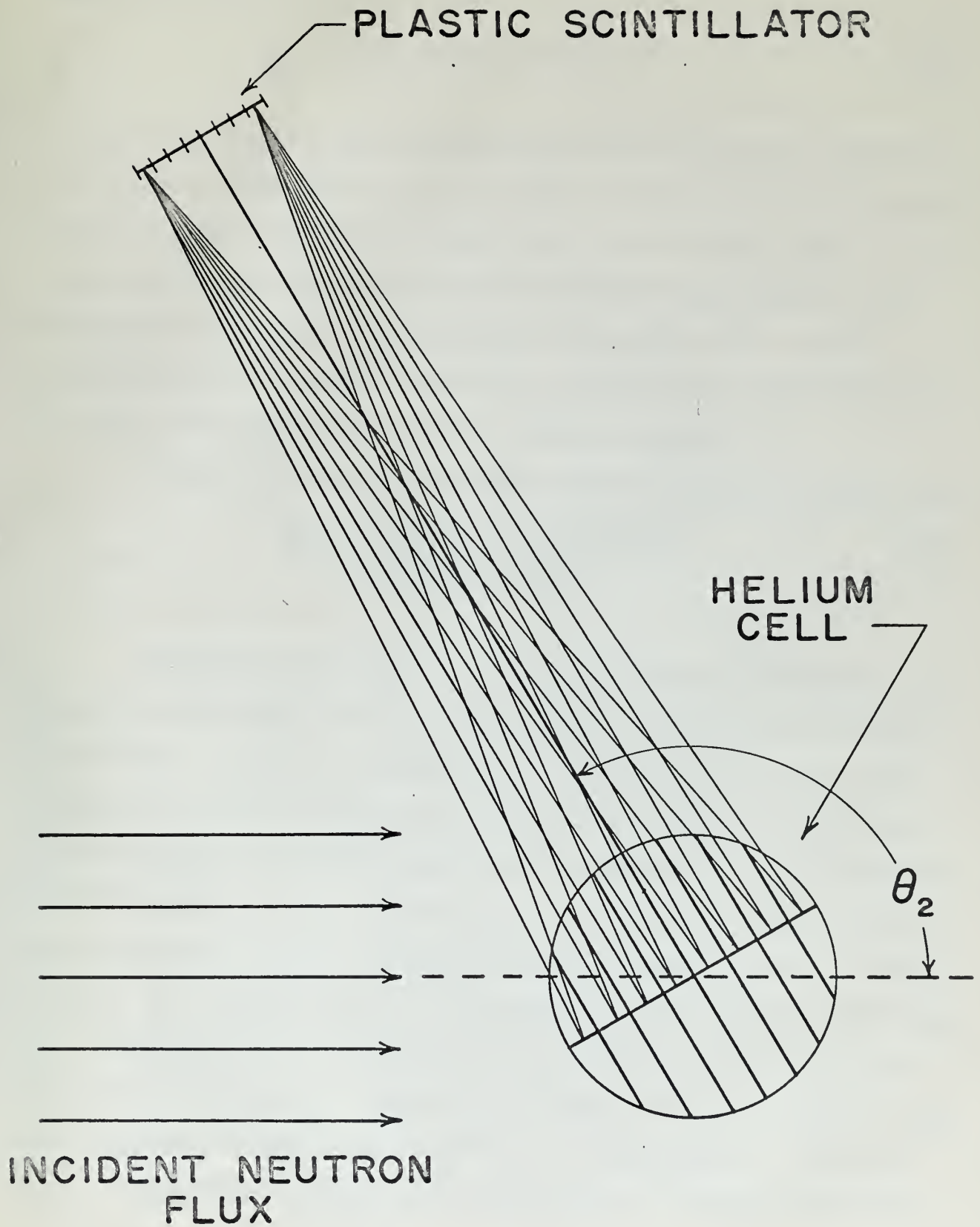
PLASTIC SCINTILLATOR
HELIUM CELL
θ_2
INCIDENT NEUTRON FLUX

Since the areas of the detector segments also were equal,

$$f_{ij} = k' \times \text{volume (i)} \times \exp(-\ell_i/\lambda). \tag{17}$$

Because the differential cross section was considered separately, the neutrons scattered from cell zone "i" have an equal probability on a geometric basis of going into any detector zone. A histogram was constructed showing the geometric probability for a neutron's scattering through θ_2 as a function of θ_2, and a smooth curve was drawn through it. Values of the geometric factor were then determined from the smooth curve.

Having determined these quantities, $\overline{P}_2$ was evaluated from

$$\overline{P}_2 = \frac{\sum_i P_{2,i}(\theta_2)\sigma_i(\theta_2) f_i(\theta_2)\eta_i(E_n)}{\sum_i \sigma_i(\theta_2) f_i(\theta_2)\eta_i(E_n)} . \tag{18}$$

Multiple scattering in the plastic scintillators was considered because its effect is to increase the efficiency nonlinearly which in turn influences $\overline{P}_2$. The total light output produced by a neutron interaction in the scintillator is increased when a neutron is doubly scattered from protons. This is particularly important when a bias is used because some scintillations which otherwise might be biased out may be raised above the bias energy. To determine whether corrections for multiple scattering were required, $\overline{P}_2$ was computed at $\theta_2 = 100^0$ and 120^0 for three efficiency conditions. The efficiency was determined for the two bias conditions which were used in the experiment, B = 165 keV and B = 250 keV; thirdly, the efficiency was taken to be unity.

If $\bar{F}_2$ is not a rapidly varying function of efficiency there is no need to correct for multiple scattering. The result of computing $\bar{F}_2$ for these three cases was that the maximum difference in $\bar{F}_2$ at any particular energy was 1 part in 190. Since F_2 is not known to this accuracy, it was not deemed worthwhile to correct for multiple scattering in the detectors.

To facilitate the computation of a multiple scattering correction for the neutrons in the helium cell, the standard assumption that all the first scatterings took place at the center of a spherical cell was made. When the attenuation of the neutron flux through the scatterer is not large, such as in the present case, this assumption is reasonable. The cell was divided into twenty-four bins in which second scattering might occur. It first was determined whether those neutrons which were scattered from the center into a given bin and then scattered a second time into the detector would satisfy the helium cell and detector energy requirements. When the requirements were satisfied, an effective value of F_2 was computed for neutrons multiply scattered from this particular bin. The corrected value of $\bar{F}_2$ was evaluated from

$$\bar{F}_2 = (F_{ss} + \sum_i F'_i r_i)/(1 + \sum_i r_i) \qquad (19)$$

where F_{ss} is the value of $\bar{F}_2$ computed assuming only single scattering occurred, F'_i is the value of F_2 for neutrons multiply scattered from zone "i" (APPENDIX), r_i is the ratio of the multiple scattered neutron intensity from zone "i" to the single

scattered intensity. The results of these computations corresponding to E_p = 3.4 MeV for the specific case discussed in the appendix are shown in Table 1. The maximum effect of multiple scattering is to lower $\overline{F}_2$ by less than 0.002 while the minimum effect is to reduce this value by less than 0.001. Since this correction is negligible compared to the value of $\overline{F}_2$ which averaged about 0.55, the calculation was not pursued further. No other corrections were determined for the value of $\overline{F}_2$.

Determination of True Asymmetry

Values of the measured asymmetry had to be corrected for background contributions from four sources. Two of these sources were cell-scattered chance and floor-scattered chance. The sum of these two sources was measured by a Type I measurement which consisted of inserting a 70 nsec delay line in the cable from the helium cell to the fast coincidence circuit. Because the resolving time of the circuit is about 10 nsec, this had the effect of putting the true counts out of coincidence, and only random counts would be recorded. Direct neutron counts were eliminated by blocking the core of the solenoid with paraffin plugs in a Type II measurement. This yielded the sum of floor-scattered normal and floor-scattered chance. The 70 nsec delay was inserted again with the plugs in place (Type III) to measure the floor-scattered chance counts alone. Other background sources were considered in a Type IV measurement with a blank Ta end cap in place. The total background to be subtracted is

Table 1

Multiple Scattering in the Helium Cell

Zone	Neutron Detector Req. Sat.	Helium Cell Req. Sat.	$r \times 10^3$	P'
1	yes	yes	0.124	0.53
2	yes	yes	0.132	0.30
3	yes	yes	0.160	0.53
4	yes	yes	0.160	0.53
5	yes	no	———	———
6	yes	yes	0.142	0.55
7	yes	yes	0.120	0.55
8	yes	yes	0.120	0.55
9	yes	yes	0.163	0.55
10	yes	yes	0.101	-0.18
11	yes	yes	0.126	0.35
12	yes	yes	0.126	0.35
13	yes	no	———	———
14	yes	yes	0.224	-0.22
15	yes	yes	0.115	0.60
16	yes	yes	0.115	0.60
17	yes	yes	0.355	0.45
18	yes	yes	0.120	0.15
19	yes	yes	0.070	0.55
20	yes	yes	0.070	0.55
21	yes	yes	0.016	0.80
22	yes	yes	0.065	0.80
23	yes	yes	0.056	0.60
24	yes	yes	0.056	0.60

BKGND = Type I + Type II - Type III + Type IV.

The average value of the total background was 5.5 percent, and the highest value was only 7.5 percent at E_p = 3.0 MeV with $\theta_2 = 120^\circ$. Total background consisted of approximately equal contributions from Type I and Type II with other sources being almost negligible. The polarization of the background was consistent with zero.

In most cases the resolving power was not sufficient to separate completely the neutrons which leave Be^7 in the ground state from those which leave it in the first excited state (Figure 10). Since the purpose of this work was to measure the polarization of only the ground-state group, separation was desirable. To eliminate the effect of the first-excited-state group, which comprise about 15 percent of the flux, a plot of the asymmetry as a function of the lower cutoff channel in the integrated pulse-height spectrum was made. The first-excited-state group has less energy than the ground-state group of neutrons so that as the lower cutoff channel is raised, the first-excited-state group should be eliminated. Because this group is known to have a low polarization, one expects that the asymmetry would rise and then level off as these neutrons are eliminated (Figure 11). Only the channels which excluded this group were included in the determination of the values of P_1P_2. The value of the plateaus in the figure were taken to be the asymmetry for the ground-state group.

The experimental and calculated results are presented in Table 2. In this table the spread of proton energies is indicated

Figure 10

Pulse-Height Spectrum of the Helium Recoils in the Helium Cell. The inability of the helium cell to resolve the two neutron groups is apparent. Because the cell was subject to total cell irradiation, the resolution (defined in Chapter III) is poorer than when it was determined for a point alpha source.

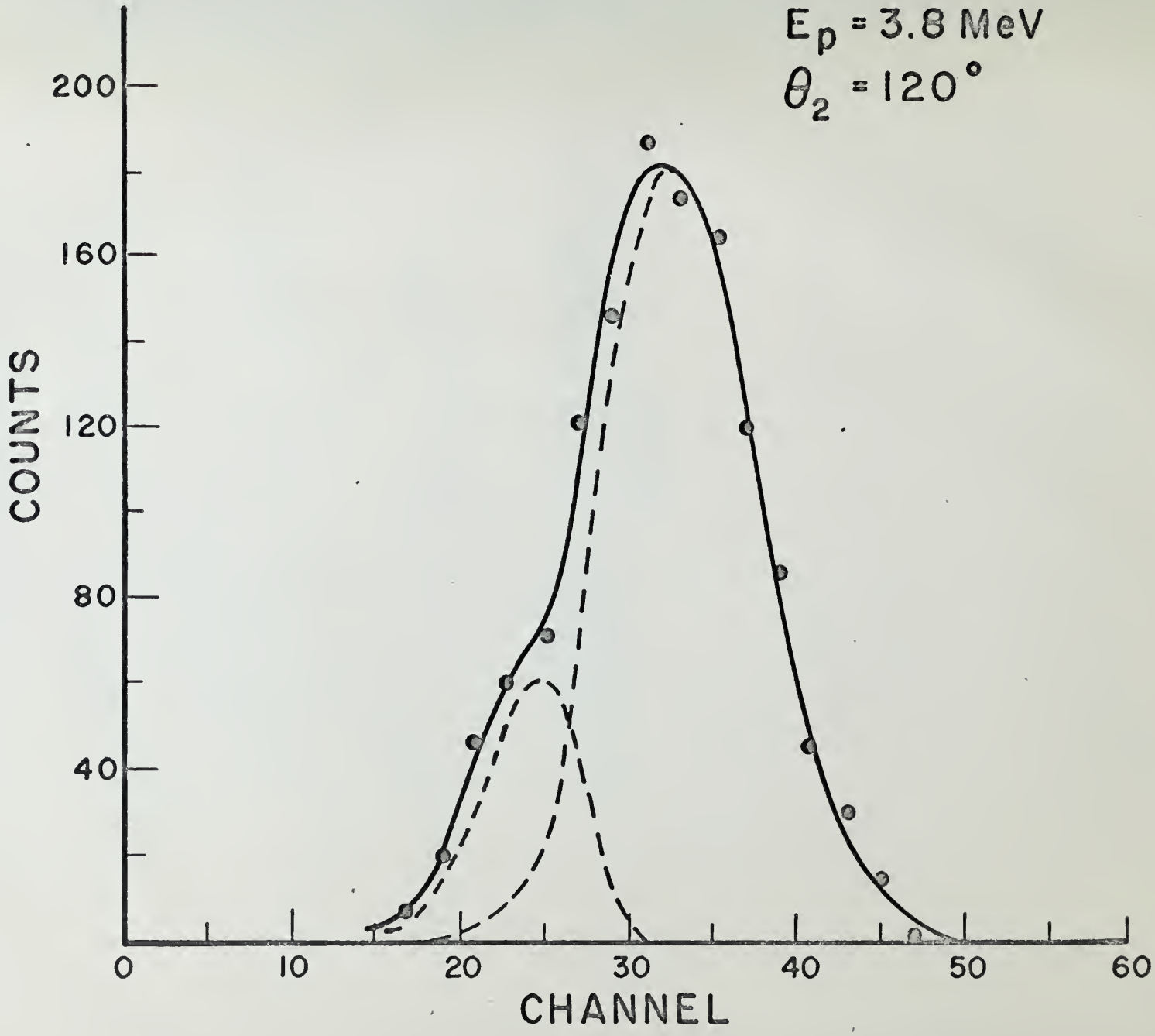
E_p = 3.8 MeV
θ_2 = 120°
COUNTS
200
160
120
80
40
0
10
20
30
40
50
60
CHANNEL

Figure 11

Elimination of the First-Excited-State Group of Neutrons from the Asymmetry.

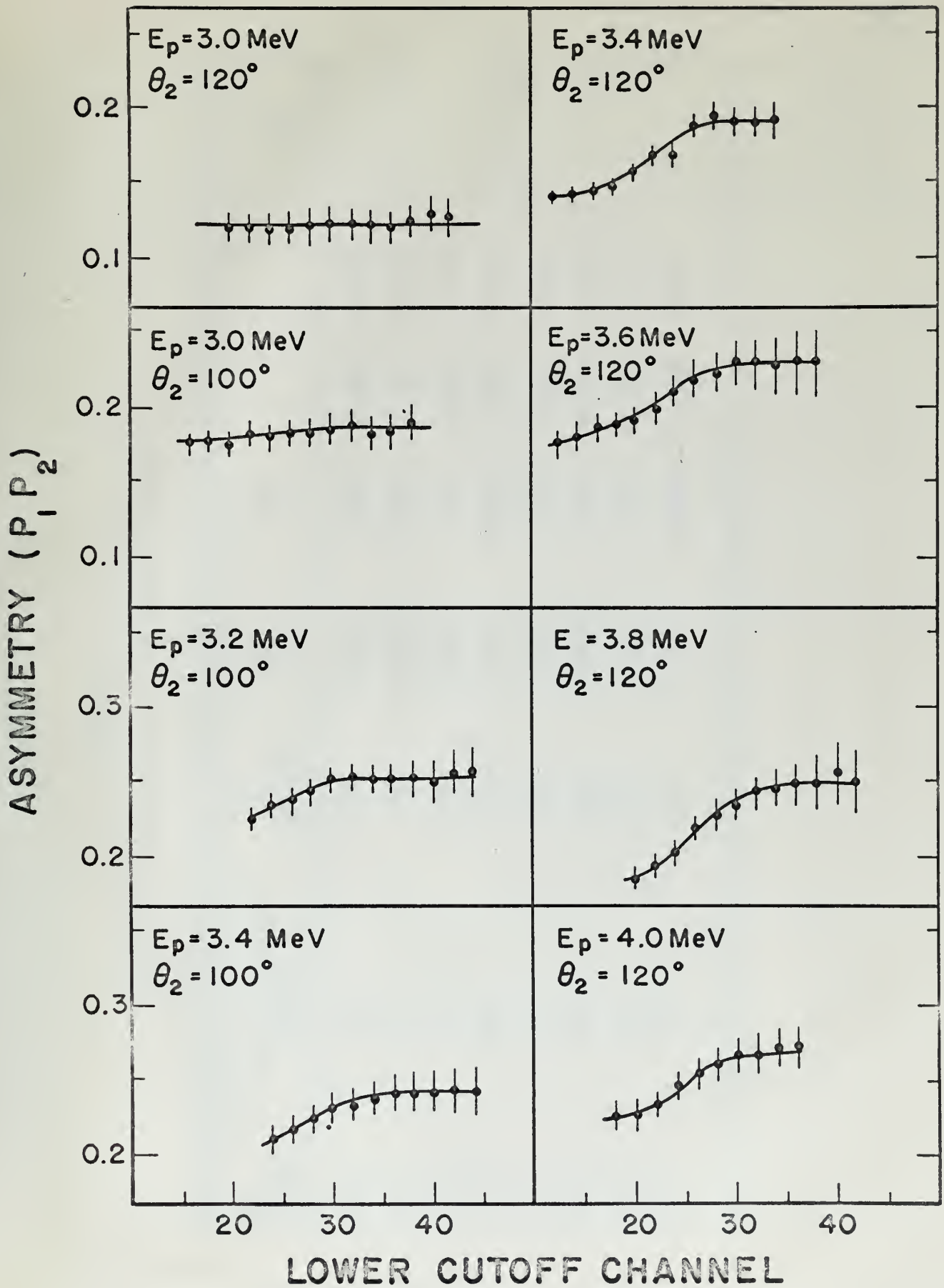
E_p=3.0 MeV
θ_2=120°
E_p=3.4 MeV
θ_2=120°
E_p=3.0 MeV
θ_2=100°
E_p=3.6 MeV
θ_2=120°
E_p=3.2 MeV
θ_2=100°
E =3.8 MeV
θ_2=120°
E_p=3.4 MeV
θ_2=100°
E_p=4.0 MeV
θ_2=120°
0.2
0.1
0.2
0.1
0.3
0.2
0.3
0.2
20
30
40
20
30
40
ASYMMETRY ($P_1 P_2$)
LOWER CUTOFF CHANNEL

Table 2

Results of Measurements and Calculations

E_p (MeV)	Target Thickness (keV)	θ_2 (Deg.)	P_1P_2	P_2	P_1	$\bar{P}_1$
2.991	94	100	0.185	0.632	0.293 ± 0.025	0.306 ± 0.017
2.991	94	120	0.122	0.383	0.319 ± 0.025	
3.196	66	100	0.248	0.699	0.355 ± 0.015	
3.377	115	100	0.230	0.733	0.323 ± 0.021	0.331 ± 0.015
3.377	77	120	0.187	0.550	0.340 ± 0.021	
3.576	55	120	0.230	0.616	0.374 ± 0.019	
3.776	92	120	0.246	0.669	0.368 ± 0.015	
3.985	75	120	0.267	0.722	0.369 ± 0.015	

by the target thickness--the energy loss of protons of energy E_p in passing through the Li. Here, E_p is the average proton energy for the measurement. The values of P_1P_2 have been corrected for background and the effects of the first-excited-state group of neutrons.

Chapter V

DISCUSSION AND CONCLUSIONS

The results of the present measurement are plotted on Figure 12 along with the results of previous experimenters for ease of comparison. A smoothly varying and generally increasing value of polarization as the energy increases is indicated by the results. Qualitatively the smooth variation agrees with that which would be expected since there are no narrow resonances in the reaction cross section in this region.

The uncertainties which are quoted are two standard deviations associated with the counting statistics only, except at the 3.0 MeV point. Here the uncertainty quoted is greater than the statistical one alone. At this energy three independent series of measurements were made of the asymmetry. First the asymmetry was determined with an analyzing angle of 100^0, then at 120^0, and thirdly again at 100^0. The associated polarization of the neutrons P_1 for the latter two series agreed quite well. However, the value of the asymmetry measured in the first series at 100^0 differed from that of the third series at 100^0 by 0.03 even though the individual measurements were made to a statistical accuracy of about 0.01. The reason for this deviation is not clear

Figure 12

Polarization of Neutrons in the Region E_p = 3.0 to 4.0 MeV.

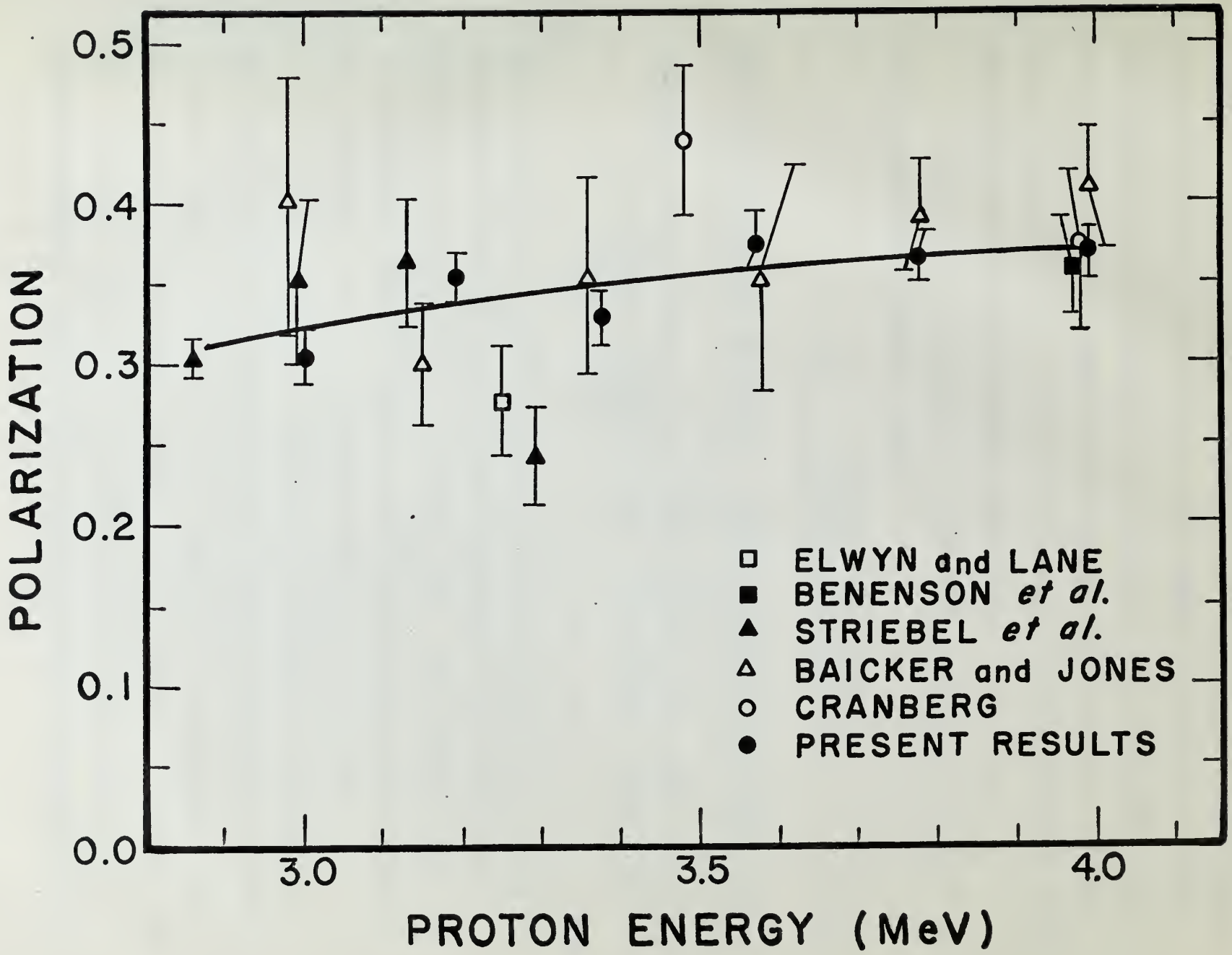
0.5
0.4
0.3
0.2
0.1
0.0
POLARIZATION
3.0
3.5
4.0
PROTON ENERGY (MeV)
ELWYN and LANE
BENENSON et al.
STRIEBEL et al.
BAICKER and JONES
CRANBERG
PRESENT RESULTS

and may be statistical in nature. To account for the possibility that the difference may be due to an unknown background or instrumental problem associated with the low neutron energies, the quoted error for the 100^0 measurement has been doubled. At the other energies where P_1 was determined at both $\theta_2 = 100^0$ and 120^0, the results were statistically consistent.

The quoted statistical errors were arrived at by the use of the expression (Orear, 1956)

$$\Delta \sigma = \sqrt{\sum_i \left(\frac{\partial \sigma}{\partial x_i}\right)^2 (\Delta x_i)^2} \quad . \tag{20}$$

Here σ is a function of the x_i. In the present work, this becomes

$$\Delta (P_1 P_2) \frac{1}{\left[1 + \left(\frac{I_{u,p}}{I_{u,a}} \times \frac{I_{d,a}}{I_{d,p}}\right)\right]} \sqrt{\frac{I_{u,p}}{I_{u,a}} \times \frac{I_{d,a}}{I_{d,p}} \left[\frac{1}{I_{u,p}} + \frac{1}{I_{d,a}} + \frac{1}{I_{d,p}} + \frac{1}{I_{u,a}}\right)} \tag{21}$$

where $P_1 P_2$ is the measured asymmetry and the I's are the intensities which have been corrected for background. The subscripts have the same meaning as in Equation (10). This assumes that the intensities are Poisson distributed which is quite realistic since the probability of an event is both small and constant.

A second source of error is that associated with P_2. It has been estimated by Haeberli (1963) that the calculated values of P_2 are known to within ten percent of the correct value. The recent measurements of May, Walter, and Barschall (1963) show that this percentage may be a conservative estimate for the present neutron energies. An indication that this source of error may be

smaller in the present experiment is the consistent value of P_1 determined at both $\theta_2 = 120^\circ$ and 100° at the 3.4 MeV point. Measurements of the value of P_2 are planned in the near future at this laboratory. At that time the uncertainty in P_2 can be evaluated more definitely. In the uncertainties quoted for P_1 in Table 2, page 51, the uncertainty in P_2 has been neglected.

Although the apparatus which was used in this experiment is adequate to determine the asymmetries which were measured, the method is limited both below proton energy 3 MeV and above 4 MeV. The upper boundary is caused by the design of the Van de Graff generator. The lower limitation is due to the low intensity of the scintillations in the helium cell. At the associated neutron energies below $E_p = 3.0$ MeV, the helium recoil pulse size is so small as to be hardly distinguishable from the large number of background pulses produced by phototube noise and gamma radiation. As the energy is lowered further, one can no longer be certain that proper neutron pulses and not background pulses are being counted.

As seen in the figure the trend of the experimental points agrees with the trend which Baicker and Jones (1960) observed, but specific values of the two experiments are sometimes quite divergent. At 4.0 MeV the results agree very well with Cranberg (1959) and Benenson *et al.* (1962). The results of Benenson *et al.* have been corrected by the author of the present paper for the effects of the first excited state group using the relative intensities of the two groups as reported by Bevington, Holland, and Lewis (1961).

As the energy is decreased, there is a general agreement until the 3.2 MeV point is reached with the exception of the Cranberg (1959) point at 3.48 MeV which is considerably higher than the overall trend. In analyzing his data, Cranberg used the values of polarization for n-He^4 scattering calculated by Levintov, Shamshev, and Miller (1957). Although an incorrect phase shift was used in their calculation, it had little effect on P_2 at the energies of Cranberg's experiment. Correcting Cranberg's value for the effect of this error does not bring it into agreement with the present results. At 3.0 and 3.2 MeV the results are lower and higher respectively than the consensus of the previous work. However the points agree well with the pattern of Striebel, Darden, and Haeberli's (1958) work below 3.0 MeV and follow the trend of slowly varying values which was expected. Evaluation of the new data relative to those of Baicker and Jonas (1960) and Striebel et al. (1958) should be tempered not only by the statistical uncertainties but also by the fact that these experimenters were operating with a background of about 50 percent whereas coincidence techniques reduced the present background to about 5 percent.

It is to be noted that all of the above experimenters used He^4 as an analyzer except Elwyn and Lane (1962) and Striebel, et al. who used O^{16}. Thus the deviation between individual points, which is noted, cannot be attributed to uncertainties in the value of P_2.

In conclusion, because the polarization of the neutrons

is high and the cross section for the reaction is large, the $Li^7(p,n)Be^7$ reaction is useful as a source of polarized neutrons. The magnitude of the polarization of neutrons emitted at an angle of 90° relative to the proton beam axis in the reaction for the region of proton energies 3 to 4 MeV is now known with relatively high accuracy. As would be expected by the lack of resonance structure in the total cross section for the reaction in this region, the polarization varies smoothly. Because these facts are now well known, the reaction is much more useful as a source of polarized neutrons at proton energies up to 4 MeV. Above this energy the neutrons are less useful because of the difficulty of resolving the two neutron groups and the decreasing magnitude of the polarization of the neutrons.

APPENDIX

APPENDIX

Multiple scattering corrections usually cannot be calculated because to do so requires a knowledge of the triple scattering parameters which are generally unknown. In the present work two of these parameters are applicable. The depolarization parameter D is related to the component of the polarization vector of the scattered neutron which is normal to the second scattering plane after the second scattering. This component will be called the D component. The rotation parameter R is a function of the magnitude of the polarization vector perpendicular to both the vector describing the second scattering plane and the momentum vector of the neutron after this scattering. This component will be referred to as the R component.

For the case in which the second scattering in the helium cell is in a plane parallel to the second scattering plane, the D component of the polarization is effective. The asymmetry is given by (Wolfenstein, 1954)

$$\epsilon_3 = P_3(P_2 + D P_1)/(1 + P_1 P_2) \qquad (22)$$

where P_3 is the polarization associated with the third scattering, P_2 with the second, and P_1 with the neutron producing reaction.

Because in the case of scattering from spin-zero nuclei the magnitude of the polarization parallel to $\vec{n}_2$ is not changed, the depolarization parameter D is unity (Wolfenstein, 1954). For this case Equation (22) becomes

$$\epsilon_3 = P_3(P_2 + P_1)/(1 + P_1P_2) \quad . \tag{23}$$

The effective analyzing power for a neutron multiply scattered in this plane is

$$P' = \epsilon_3/P_1 \quad . \tag{24}$$

If the second scattering in the helium cell is in a plane normal to $\vec{n}_2 \times \vec{k'}_n$, the asymmetry is (Wolfenstein, 1954)

$$\epsilon_3 = P_3(\theta_3)P_1R \tag{25}$$

where θ_3 is the angle described by $\vec{k'}_n$ and $\vec{k''}_n$ which are the momentum vectors of the singly scattered and multiply scattered neutrons respectively. Because of the difficulty of the computations required to evaluate the R parameter for all angles, it was not calculated for the present corrections. The maximum and minimum effects of multiple scattering which correspond to the limiting values of R, - 1 and + 1 respectively, were determined. Table 1, page 45, shows the values of P' when R is + 1. Further and much more detailed work on multiple scattering will be done in the near future in conjunction with the same experiment referred to on page 57. The effective analyzing power again is given by Equation (24) with the asymmetry given by Equation (25).

The correction to F_2 was determined by dividing the cell into twenty-four bins in such a manner that the center of each lay in a plane either parallel or perpendicular to the second scattering plane. It was assumed that all the multiple scatterings in a given bin took place at the center of the bin. Having determined P', the correction to F_2 was computed as described in Chapter III. The corrections determined in this manner were of such low magnitude (page 44) that more detailed calculations were deemed unnecessary at this time.

LIST OF REFERENCES

LIST OF REFERENCES

R.K. Adair, S.E. Darden, and R.E. Fields, Phys. Rev. 96, 503 (1954).

J.A. Baicker and K.W. Jones, Nucl. Phys. 17, 424 (1960).

W. Benenson, T.H. May, and R.L. Walter, Nucl. Phys. 32, 510 (1962).

H.A. Bethe and P. Morrison, Elementary Nuclear Theory, 2nd. ed. (John Wiley & Sons, Inc., New York, 1956), Chap. XVII, p. 133.

P.R. Bevington, W.W. Roland, and H.W. Lewis, Phys. Rev. 121, 871 (1961).

L. Cranberg, Phys. Rev. 114, 174 (1959).

R.M. Eisberg, Fundamentals of Modern Physics (John Wiley & Sons, Inc., New York, 1961), Chap. 16, p. 602.

W.C. Elmore and M. Sands, Electronics (McGraw-Hill Book Co., Inc., New York, 1949).

A.J. Elwyn and R.O. Lane, Nucl. Phys. 31, 78 (1962).

A.J. Elwyn, R.O. Lane, A. Langsdorf, Jr., and J.E. Monahan, Phys. Rev. 133, B 80 (1964).

W.S. Emmerich, Fast Neutron Physics, ed. by J.B. Marion and J.L. Fowler (Interscience Publishers, New York, 1963), Part II, Chap. V.C.

J.H. Gibbons and H.W. Newson, Fast Neutron Physics, ed. by J.B. Marion and J.L. Fowler (Interscience Publishers, New York, 1960), Part I, Chap. I.E.

W. Haeberli, Fast Neutron Physics, ed. by J.B. Marion and J.L. Fowler (Interscience Publishers, New York, 1963), Part II, Chap. V.G.

P. Hillman, G.H. Stafford, and C. Whitehead, Nuovo Cimento 4, 67 (1956).

C.E. Hollandsworth, S.G. Buccino, and P.R. Bevington, Nucl. Instr. (in print).

C.M. Huddleston, Fast Neutron Physics, ed. by J.B. Marion and J.L. Fowler (Interscience Publishers, New York, 1960), Part I, Chap. III.D.

I.I. Levintov, V.N. Shamshev, and A.V. Miller, Nucl. Phys. 3, 221 (1957).

T.H. May, R.L. Walter, and H.H. Barschall, Nucl. Phys. 45, 17 (1963).

R.H. Miller, Rev. Sci. Instr. 30, 395 (1959).

J. Orear, Notes on Statistics for Physicists, (University of California Radiation Laboratory Report No. 8417 to the U.S. Atomic Energy Commission, 1958), p. 15.

M.A. Preston, Physics of the Nucleus (Addison-Wesley Publishing Co., Inc., Reading, Mass. 1962), Chap. 5, p. 86.

J.D. Seagrave, Phys. Rev. 92, 1228 (1953).

R.K. Sheline, Nucl. Instr. 14, 297 (1962).

Sign Convention for Particle Polarization, Nuc. Phys. 21, 696 (1960).

H.H. Strickel, S.E. Darden, and W. Haeberli, Nucl. Phys. 5, 180 (1958).

C.D. Swartz and C.L. Owen, Fast Neutron Physics, ed. by J.B. Marion and J.L. Fowler (Interscience Publishers, New York, 1960), Part I, Chap. II.B.

I. Tamchek and A. Nemmendinger, Phys. Rev. 74, 573 (1948).

T.A. Wilson, Fast Neutron Physics, ed. by J.B. Marion and J.L. Fowler (Interscience Publishers, New York, 1963), Part II, Chap. V.F.

H.B. Willard, J.K. Bair, and J.D. Kington, Phys. Rev. 95, 1559 (1954).

L. Wolfenstein, Phys. Rev. 96, 1654 (1954).

thesA497
Polarization of neutrons from the Li Sup
3 2768 001 07062 6
DUDLEY KNOX LIBRARY